IET Generation, Transmission & Distribution

Research Article

ISSN 1751-8687
Received on 20th May 2014
Accepted on 19th December 2014
doi: 10.1049/iet-gtd.2014.0481
www.ietdl.org

Non-invasive identification of turbo-generator parameters from actual transient network data

Greame Hutchison[1] ✉, Bashar Zahawi[2], Keith Harmer[1], Shady Gadoue[3,4], Damian Giaouris[5]

[1]*Parsons Brinckerhoff, Newcastle Business Park, Newcastle upon Tyne NE4 7YQ, UK*
[2]*Department of Electrical and Computer Engineering, Khalifa University, Abu Dhabi 127788, UAE*
[3]*School of Electrical and Electronic Engineering, Newcastle University, Newcastle upon Tyne NE1 7RU, UK*
[4]*Department of Electrical Engineering, Faculty of Engineering, Alexandria University, Alexandria 21544, Egypt*
[5]*Chemical Process Engineering Research Institute (CPERI), Centre for Research and Technology Hellas 57001 Thessaloniki, Greece*
✉ *E-mail: HutchisonG@pbworld.com*

Abstract: Synchronous machines are the most widely used form of generators in electrical power systems. Identifying the parameters of these generators in a non-invasive way is very challenging because of the inherent non-linearity of power station performance. This study proposes a parameter identification method using a stochastic optimisation algorithm that is capable of identifying generator, exciter and turbine parameters using actual network data. An eighth order generator/turbine model is used in conjunction with the measured data to develop the objective function for optimisation. The effectiveness of the proposed method for the identification of turbo-generator parameters is demonstrated using data from a recorded network transient on a 178 MVA steam turbine generator connected to the UK's national grid.

1 Introduction

The accurate modelling of synchronous machines, excitation systems and prime movers to predict power station performance is clearly a very important topic that has been the subject of interest for several decades. The most accurate method of establishing generator armature and field windings parameters is through a standstill resistance test [1], but this has the inherent disadvantage that the test has to be performed at standstill. The more common method for calculating the values of machine parameters is therefore to perform the usual short circuit and open circuit tests and use the results to calculate the various machine parameters. The major drawback with this method is its invasive nature in regard to testing. This is not a practical proposition when considering network connected generators.

Parameter identification has also been attempted using differing methods to produce representations of the armature and the rotor field windings. Parameter estimation of the electrical *d-q* axis equivalent circuit of a 7 kVA synchronous generator has been carried out using a standstill time-domain test based on applying a sine cardinal perturbation voltage signal in conjunction with GA and a Gauss–Newton technique [2]. Another perturbation method based on generating multisinusoidal excitation signal using a pulse width modulation voltage source inverter has been described in [3]. Work has also been carried out to identify the parameters of a saturated synchronous machine model using a small 3 kVA synchronous generator by performing a full load rejection test [4]. Synchronous machine parameter estimation using a line-to-line short circuit test has also been carried out [5]. Parameter identification for excitation systems has also been attempted, generally performed using step response tests to ascertain the system's base function under perturbation [6]. This form of identification is performed using the exciter in a standalone format and without direct synchronous machine interaction. Online estimation of the synchronous generator parameters has been also considered [7–9] to provide continuous update of the machine parameters during operation. Invariably these identification methods consider machine electrical parameters only and are simulation based or require an instigated perturbation or signal disturbances around an operating point which may require expensive signal generation equipment [2, 3, 8, 10, 11].

Much like the identification of machine and exciter parameters, gas and steam turbines have been accurately characterised over the years. This work, however, has been considered largely from a thermodynamic perspective [12] and required significant specification data to produce an accurate picture of the turbine performance. These detailed models are invariably too complex to be used in a turbo-generator parameter identification study.

This paper demonstrates a different approach for turbo-generator parameter identification including generator, excitation system and prime mover variables, based on the use of recorded data from an actual network transient, without the need for special tests or signal injection techniques. The proposed method utilises a classical synchronous machine model [13, 14]. An adaptable excitation system model [6] is utilised to model field voltage control and a standard, industrially accepted turbine model is utilised to characterise prime mover function [15]. A real recorded transient event occurring at some distance from a 178 MVA generator is then used as the basis for a totally non-invasive optimisation procedure to identify generator, exciter and turbine parameters in one process.

2 Generator, exciter and turbine models

The classical dynamic model of a synchronous machine is given by the following equations in the rotor *dq* reference frame in which only one field winding in the *d*-axis and a pair of damper windings in the *d*-axis and the *q*-axis are present and the voltage equations are expressed as integral equations of the flux linkages in the machine windings [14]

$$\psi_q = \omega_b \int \left\{ V_q - \frac{\omega_r}{\omega_b}\psi_d + \frac{R_s}{X_{ls}}(\psi_{mq} - \psi_q) \right\} dt \qquad (1)$$

$$\psi_d = \omega_b \int \left\{ V_d - \frac{\omega_r}{\omega_b}\psi_q + \frac{R_s}{X_{ls}}(\psi_{md} - \psi_d) \right\} dt \qquad (2)$$

$$\psi_0 = \omega_b \int \left\{ V_0 - \frac{R_s}{X_{ls}} \psi_0 \right\} dt \tag{3}$$

$$\psi_{kq} = \frac{\omega_b R_{kq}}{X_{lkq}} \int (\psi_{mq} - \psi_{kq})\, dt \tag{4}$$

$$\psi_{kd} = \frac{\omega_b R_{kd}}{X_{lkd}} \int (\psi_{md} - \psi_{kd})\, dt \tag{5}$$

$$\psi_f = \frac{\omega_b R_f}{X_{md}} \int \left\{ E_f - \frac{X_{md}}{X_{lf}} (\psi_{md} - \psi_f) \right\} dt \tag{6}$$

where ψ_d, ψ_q, ψ_0 are the stator windings flux linkages, ψ_f is the field winding flux linkage, ψ_{kd} is the d-axis damper winding flus linkage, ψ_{kq} is the q-axis damper windings flux linkage and ψ_{md}, ψ_{mq} are the mutual flux linkages in the d-axis and q-axis circuits, respectively. ω_b and ω_r are the base electrical angular speed and the rotor angular speed, respectively. R_s is the stator winding resistance, R_f is the field winding resistance, R_{kd} is the d-axis damper winding resistance and R_{kq} is the q-axis damper windings resistance. X_{ls} is the stator winding leakage reactance, X_{lf} is the field winding leakage reactance, X_{lkd} is the d-axis damper winding leakage reactance, X_{lkq} is the q-axis damper winding leakage reactance and X_{md} is the d-axis stator magnatising reactance. V_d, V_q, V_0 are the network voltages and E_f is given by the equation

$$E_f = X_{md} \frac{V_F}{R_f}$$

where V_F is the voltage regulator output.

The mutual fluxes ψ_{md}, ψ_{mq} are given by

$$\psi_{mq} = \omega_b L_{mq}(i_q + i_{kq})$$
$$\psi_{md} = \omega_b L_{md}(i_d + i_{kd} + i_f)$$

Having determined the values of the various flux linkages, we can then calculate the winding currents using the equations

$$i_q = \frac{\psi_q - \psi_{mq}}{X_{ls}} \tag{7}$$

$$i_d = \frac{\psi_d - \psi_{md}}{X_{ls}} \tag{8}$$

$$i_{kd} = \frac{\psi_{kd} - \psi_{md}}{X_{lkd}} \tag{9}$$

$$i_{kq} = \frac{\psi_{kq} - \psi_{mq}}{X_{lkq}} \tag{10}$$

$$i_f = \frac{\psi_f - \psi_{md}}{X_{lf}} \tag{11}$$

The stator winding currents i_a, i_b, i_c can then be obtained using the reverse *dq/abc* transformation.

The electromechanical torque developed by the machine, T_e, is then given by

$$T_e = \frac{3}{2} \frac{p}{\omega_b} (\psi_d i_q - \psi_q i_d) \tag{12}$$

where p is the number of pole pairs.

The above standard equations are developed in motoring convention, that is, with the positive direction of current defined as entering the positive polarity of the winding terminal voltage. The value of T_e obtained from (12) is therefore positive for motoring operation and negative for generating operation. For a synchronous generator, the mechanical equation of motion can thus be written as

$$T_{mech} + T_e - T_{damping} = 2H \frac{\partial[\omega_r/\omega_b]}{\partial t} \tag{13}$$

where T_{mech} is the mechanical torque developed by the prime mover, $T_{damping}$ is the system damping torque and H is the inertia constant of the generator.

It must be noted here that the parameters of the standard machine (1)–(13) used in the analysis are not in a form which relates directly to the machine and system parameters supplied by machine manufacturers that are the subject of the parameter identification process described in this paper (see Table 1). The two sets of parameters are however related by a standard set of equations as described in the Appendix.

The excitation system control is formulated using an AC5A exciter model (Fig. 1) in which the synchronous machine excitation control system is made up of several subsystems [6] that may include a terminal voltage transducer, an excitation controller, as well as the exciter itself. In this model, V_C is the output of the terminal voltage transducer, V_{REF} is the regulator reference voltage, V_R is the regulator output voltage, V_F is the exciter output voltage, K_A is the voltage regulator gain, K_E is the exciter constant, K_F is the excitation control system gain, T_A is the voltage regulator time constant, T_E is the exciter time constant and T_F is the excitation control system time constant. The AC5A has been shown to be capable of characterising different forms of exciters with a reasonable level of accuracy [6]. An exciter model of this type has the advantage of not requiring the field current to be used as a feedback signal during simulation. This is beneficial as generation stations do not have current transformers with a sufficiently high time resolution on the field windings as a matter of course. The saturation term S_E for the excitation system is characterised using a generic value ($S_E = 0.86$) obtained from IEEE Std 421–2005.

The turbine/governor model is shown in Fig. 2. The model [15] is developed using the speed deviation between the actual rotor speed and system frequency $\Delta\omega$ as its main input. In this model, P_0 is the initial mechanical power, K is the total effective governor system gain, T_1, T_2 and T_3 are the governor system time constants and

Table 1 Results of the first stage of parameter identification; generator and turbine parameters

Parameter	Manufacturer data	Identified value
R_s armature resistance, pu	0.0048	0.0054
X_d d-axis reactance, pu	1.68	1.66
T'_d transient time constant, s	0.83	0.71
X'_d transient d-axis reactance, pu	0.301	0.302
X'_d sub-transient d-axis reactance, pu	0.238	0.253
X_q q-axis reactance, pu	1.65	1.70
T''_d sub transient time constant, s	0.0035	0.0989
H Inertia Constant, pu	3.74	3.42
X'_q sub-transient q-axis reactance, pu	0.228	0.249
T''_q sub transient time constant, s	0.035	0.030
K_1Turbine gain, pu	unknown	1.03
T_4 turbine time constant, s	unknown	0.657

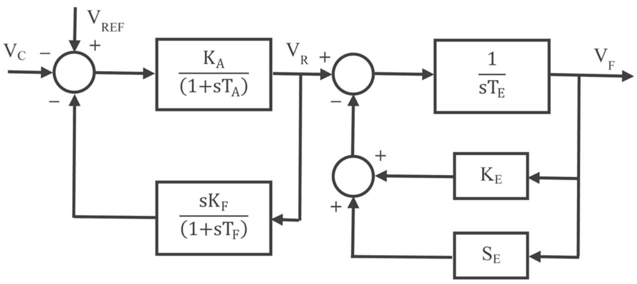

Fig. 1 *AC5A excitation system model*

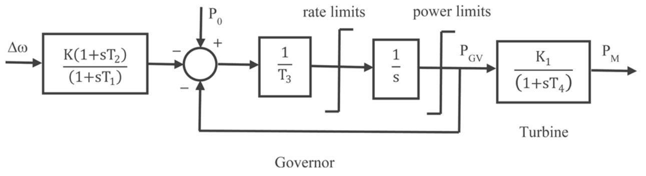

Fig. 2 *Turbine/governor model*

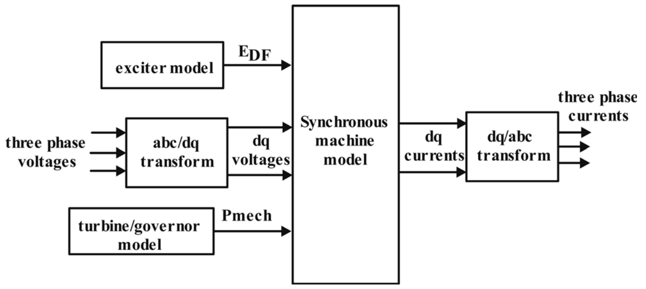

Fig. 3 *Model structure*

P_{GV} is the governor output power which is used to drive the turbine representation in the model in which K_1 is the turbine system gain and T_4 is the turbine system time constant. More general forms of turbine model capable of characterising differing prime mover types are given in [15, 16]. A more advanced model capable of modelling fast valving is available [17] but was not used in this study because of the nature of the steam turbine utilised in this work.

The different component models are combined together to form the larger system model shown in Fig. 3. The rotor block input is characterised as a mechanical torque equated to the mechanical output from the turbine model. Recorded three phase voltages are converted into *dq* quantities and used as input variables. The output of the machine model is in the form of *dq* currents. These are transformed back into their natural *abc* frame of reference and used in the following sections as the basis of the objective function for optimisation.

3 Particle swarm optimisation (PSO) algorithm

PSO is used in this study as the stochastic optimisation tool. The algorithm has been successfully employed in the past for a number of applications including power systems [18–21], power electronics [22], machine design optimisation and development of their mathematical models [23, 24] and parameter identification [25–27].

PSO is a cooperative population based stochastic search optimisation algorithm which uses evolutionary operations to mimic the behaviour of groups of animals in social activities where multi-lateral group communication is needed. The individual animals are characterised as particles, all with certain velocities and positions in the search space. The group of particles is classed as a swarm. The swarm generally begins with a randomly initialised population, each particle flying through the search space and remembering its optimal position thus far. The particles communicate with each other and based on the best positions found, dynamically adjust the search position and relative velocity of the swarm. The equations that define the PSO's behaviour are

$$v_i^{(k+1)} = K\left\{w_i v_i^k + [c_1 r_1(p_\mathrm{b} - x_i^k)] + [c_2 r_2(g_\mathrm{b} - x_i^k)]\right\} \tag{14}$$

$$x_i^{(k+1)} = x_i^k + v_i^{(k+1)} \tag{15}$$

where x_i^k is the position of the *i*th particle after *k* iterations and v_i is the velocity of particle x_i.c_1 and c_2 are positive constants referred to as the acceleration coefficients, p_b is the best previous position of particle x_i, g_b is the best previous position among all the members of the population, r_1 and r_2 are random numbers between 0 and one representing the weight the particle gives to its own previous best position and that of the swarm and w is an inertia weighting factor. Using these two equations, the position of each particle is evolved to a new position in the solution space until the optimum solution is obtained. One other aspect used in this study that is not common to other examples of PSO for parameter identification purposes is the use of the constriction factor K in (14). This factor limits the search space per iteration [28] increasing the speed and likelihood of convergence. The constriction factor is a constant and the value used is calculated from the values of c_1 and c_2

$$K = \frac{2}{|2 - \sigma - \sqrt{\sigma^2 - 4\sigma}|} \tag{16}$$

where $\sigma = c_1 + c_2$ and $\sigma > 4$.

To make the search as efficient as possible, boundary conditions are implemented to constrain each parameter to within a range of practical values. In doing this the PSO search algorithm has a limited search area, which significantly increases is speed of convergence. In this study, boundary conditions are applied using interval confinement as shown

$$x_i \notin [x_{\min}, x_{\max}] \begin{pmatrix} v_i \leftarrow 0 \\ x_i < x_{\min} \Rightarrow x_i \leftarrow x_{\min} \\ x_i > x_{\max} \Rightarrow x_i \leftarrow x_{\max} \end{pmatrix}$$

The swarm of particles moves around the search space looking for better locations than have been previously found. Through the many iterations of the search, the algorithm identifies successive combinations of parameter values that produce an improvement in the objective function error. This improvement in location translates to a more accurate set of parameter values as the process continues. Ultimately, the search algorithm proceeds to find an appropriate value for each of the parameters at which point the error is small enough to satisfy convergence criteria.

4 Recorded network transient

The transient dataset utilised in this study is that of an external phase to phase fault on the UK supply network, as shown in Figs. 4 and 5. The network transient is from a 178 MVA 2-pole, 18 kV steam turbine generator fed by a tuned AC2A pilot exciter. The generator operates with no neutral connection to ground to prevent the flow of zero-sequence currents. The data are for a real fault occurring in a real network whilst the machine is running on load. Initially it is seen that the generator is running in steady state. At 0.08 s, a phase to phase fault occurs between phases A and C at a point in the network. This fault causes the phase to neutral voltage of the faulted phases to have the same phase and magnitude as one another, as shown in Fig. 4. The voltage of the healthy phase B is displaced by 180 degrees with respect to the faulted phases and has twice the magnitude of the faulted phases so that the voltage sums to zero. The healthy phase (phase B) continues to carry current to the load as one would expect (i.e. i_B is not zero as it would be in a test with the machine running initially on open circuit). The result is that the two faulted phase currents are not equal (Fig. 5) as the three current must collectively sum to zero.

At 0.16 s the line protection trips the line and clears the fault. The under voltage protection at the generator registers the fault and trips the generator at around 0.21 s. The clearance of the fault is observed in the recovery of the phase to neutral voltage and current between 0.16 and 0.21 s. During this period both phase current and voltage are seen to recover to near steady state conditions. At 0.21 s, when the under voltage relay trips off the generator, the machine is running in an open circuit condition. Owing to this condition the phase to neutral voltage remains relatively stable whereas the phase current drops to a near zero value in all phases. The small

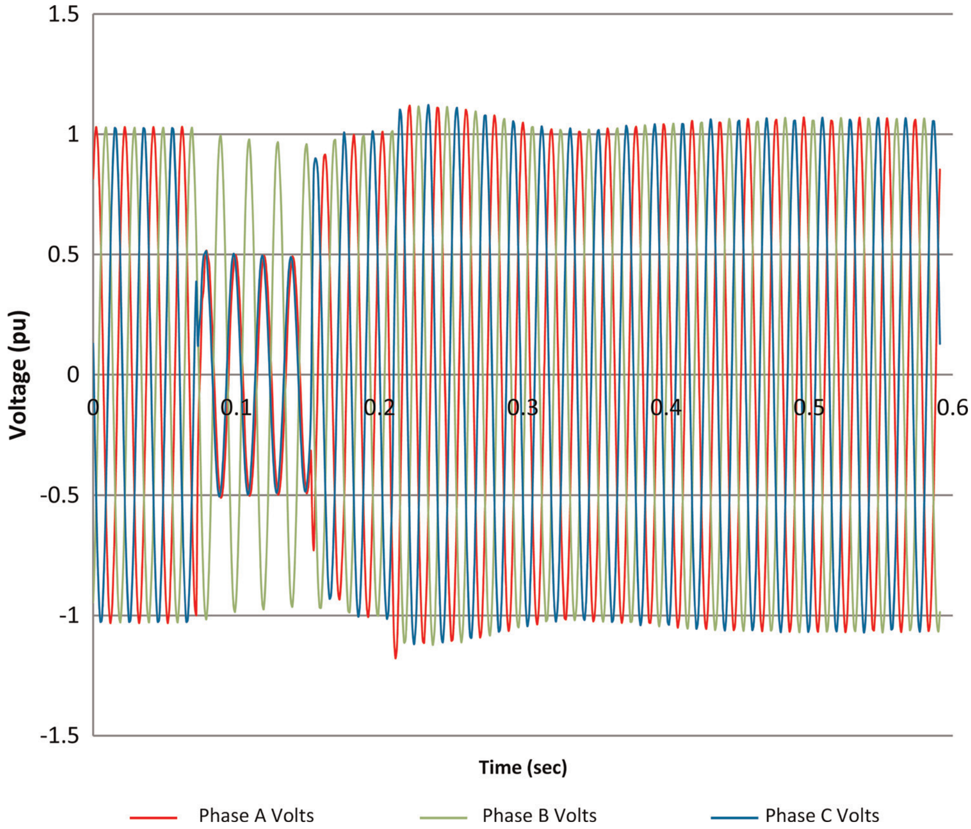

Fig. 4 *Recorded transient voltages*

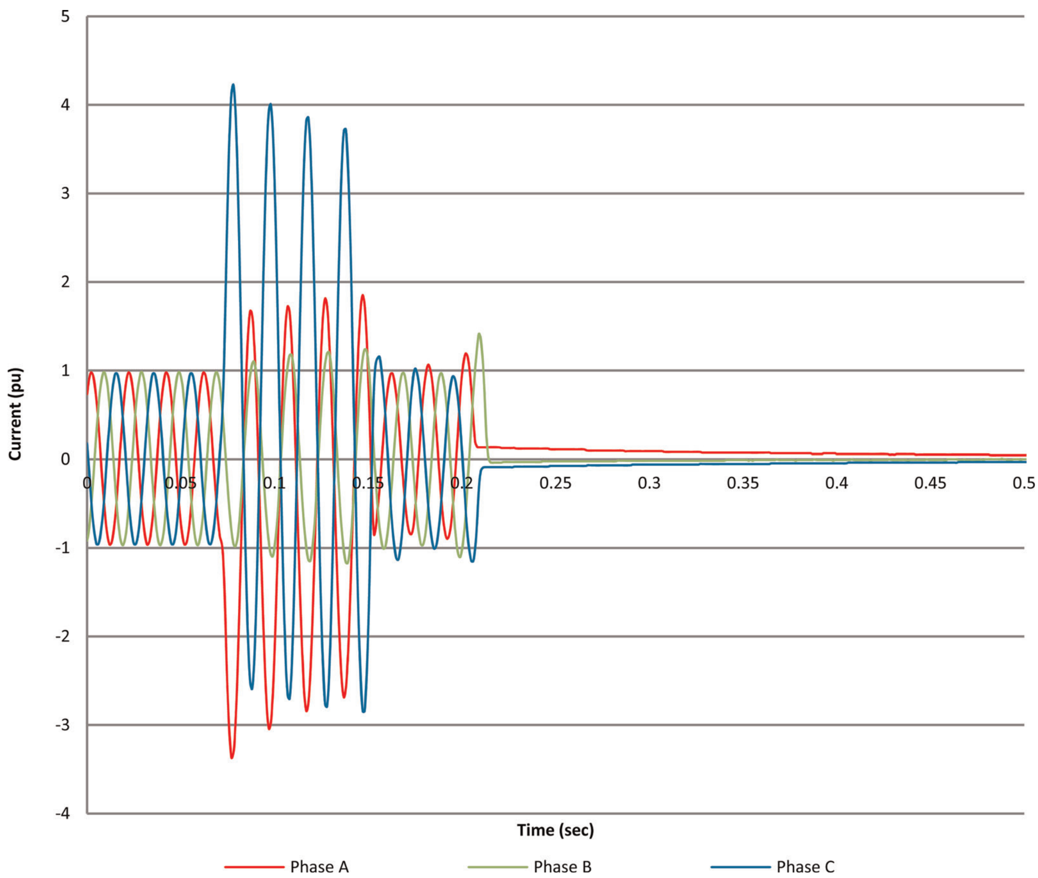

Fig. 5 *Recorded transient currents*

phase current dc offset observed in Fig. 5 from the point of tripping till around 0.7 s is the residual current in the current transformer.

5 Implementation of the parameter identification process

Fig. 6 shows a schematic representation of the parameter identification method. Using measured transient supply voltages as input variables, stator currents are calculated from the turbo generator model and compared with the actual measured currents to produce the optimisation cost function (the ‘error’ function) based on the absolute value of the errors between the two sets of currents

$$E = \sum \{|i_{am} - i_{ac}| + |i_{bm} - i_{bc}| + |i_{cm} - i_{cc}|\}\Delta T \qquad (17)$$

where (i_{am}, i_{bm}, i_{cm}) is the measured current set, (i_{ac}, i_{bc}, i_{cc}) is the calculated current set and ΔT is the sampling period.

Parameter identification is carried out by adjusting the model parameters, using the PSO algorithm to minimise the error function to within a pre-set tolerance value. The model parameters at this point match the real machine parameter values as closely as defined by the convergence criteria. The PSO algorithm was set to optimise using a swarm of 20 particles and 4 informants per iteration. Acceleration coefficients c_1 and c_2 were both set to 2.05 [Owing to the relatively high number of parameters and thus dimensions that were being searched, the choice of values of the acceleration coefficients c_1 and c_2 was severely constrained. Setting them outside of certain specific limits resulted in a search ‘explosion’ that has been documented in [29].] giving a constriction factor of 0.729. The inertia weighting was set at 0.9. A limit of 10 000 iterations was set as stop criteria for the algorithm. The convergence criterion was set to a value of objective function error of 0.0001.

In considering the transient shown in Figs. 4 and 5, it is seen that there are two distinct stages in the transient. During the first stage (the phase to phase fault), the synchronous generator characteristics have a dominant effect on the generator current waveforms. In the second part of the transient (after fault clearance and before the generator is tripped), the exciter characteristics have a significant impact on the generator waveforms. During this period, the excitation system provides maximum voltage to the field winding of the synchronous machine to prevent armature voltage depression. Fig. 7 shows a comparison of the recorded current data with those calculated from a generator model using manufacturer parameter values and a generic set of exciter parameter values [6]. It is interesting to note that the recorded current transients are lower than the currents calculated from the turbo generator model. This would indicate that the effective system parameters are in fact significantly different from those declared by the manufacturer, in agreement with previously published studies [10].

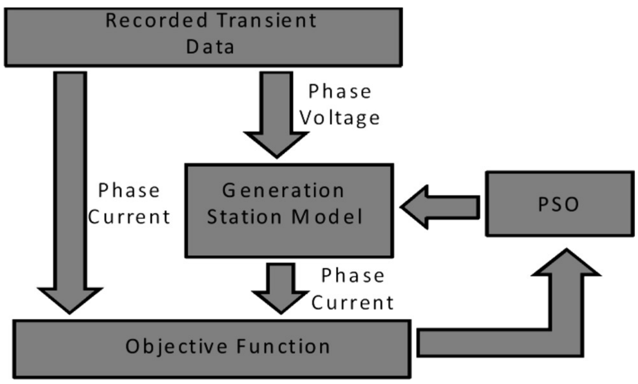

Fig. 6 *Schematic representation of the PSO search based parameter identification technique*

6 Results

When attempting to identify all the parameters (generator, turbine and exciter parameters) simultaneously (i.e. when treating the process as one optimisation study) using the entire recorded transient, the resulting algorithm absolute current error signal was relatively high. To reduce the computational burden of the algorithm and improve the accuracy of the method, a two-stage identification process is implemented in which machine and turbine parameters are identified first using the phase to phase fault data. These parameters then become the basis for the secondary stage of the process in which excitation system parameters are identified using recovery period data.

Table 1 shows the synchronous machine and turbine parameter values identified from the first stage of the search process [Repeated simulations showed that variations in governor model parameter values (k, T_1, T_2 and T_3 in Fig. 2) had little or no

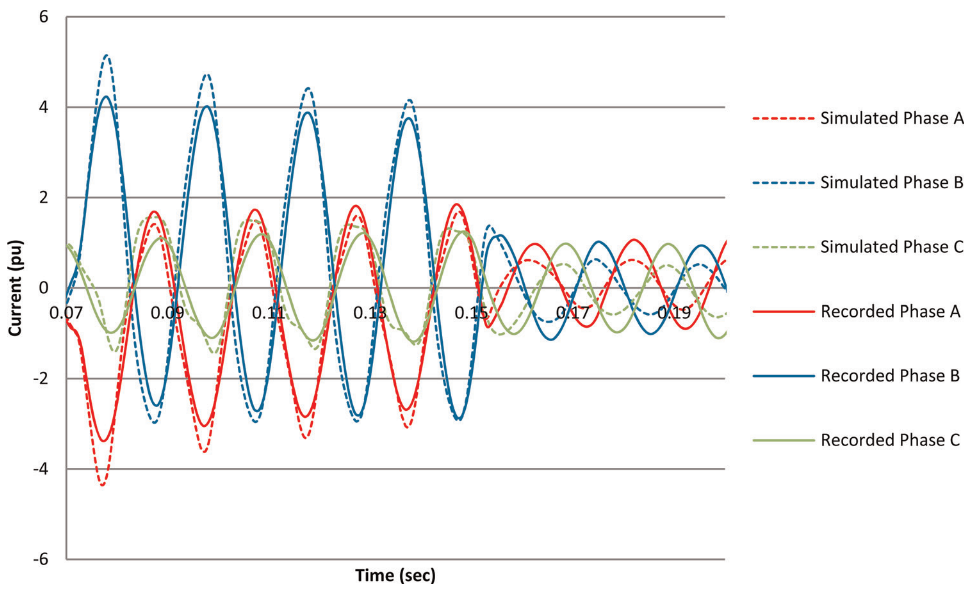

Fig. 7 *Comparison between simulated current waveforms calculated using manufacturer parameter values and the recorded transient currents*

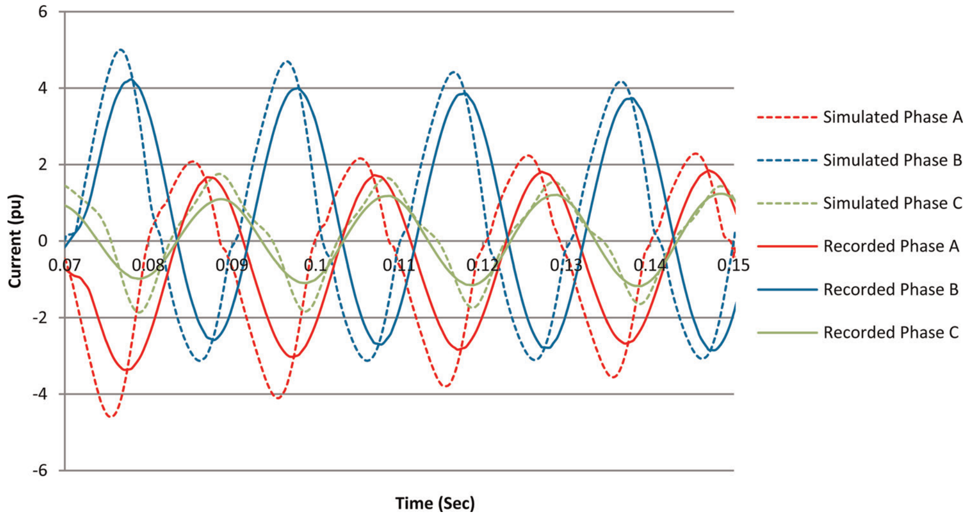

Fig. 8 *Simulated current waveforms calculated using the identified generator/turbine parameter values after the 1st stage of the process compared with the recorded transient currents*

Table 2 Results of the second parameter identification stage; exciter parameters

Parameter	Manufacturer data	Identified value
K_F, pu	0.03	0.044
K_E, pu	1	1.10
T_E, s	0.8	0.58
K_A, pu	400	457.0
T_F, s	1	0.78
T_A, s	0.02	0.021

influence on the final obtained solutions, because of the relatively large time constants compared with the short period of the fault transient. Generic values of $k = 0.95$ pu, $T_1 = 0.25$ s, $T_2 = 0$ and $T_3 = 0$ were therefore used as recommended in [14]. These parameters were then excluded from the stochastic search process.] compared against manufacturer's data. X_q is seen to give a result which is close to the manufacturer declared value. The identified values for the transient and sub transient direct axis reactances are marginally higher than manufacturer's values. This has a specific bearing on the generator response during the phase to phase fault (Fig. 8). The higher impedance values identified would reduce the calculated fault currents to a value closer to the recorded currents, reducing the discrepancy between the two sets of waveforms seen in Fig. 7. This would indicate that the manufacturer declared values have a significant degree of tolerance as suggested by previous researchers [10]. It is more difficult to quantify whether the identified turbine values are accurate because there no declared manufacturer's values are available. It can be said however that the identified parameter values are appropriate to the magnitude and type of the turbine that is being considered in this work.

Having identified the above machine and turbine parameter values, the search process is then focused on the identification of exciter model parameters using the fault recovery period of the recorded transient data. Table 2 shows results of this second stage of the parameter identification process. Fig. 9 shows the complete recorded transient current waveform compared against the generator current waveforms calculated by using the generator, turbine and excitation system parameter values identified from the multistage PSO search process.

The PSO identified parameters enable the simulated response of the synchronous generator to mirror the recorded transient data set reasonably accurately, especially during the fault recovery period. Comparing Figs. 7 and 9, it is interesting to note that the PSO identified parameters give a significant improvement in terms of matching the recorded transient during the fault recovery period but not during the initial fault period. During the fault transient

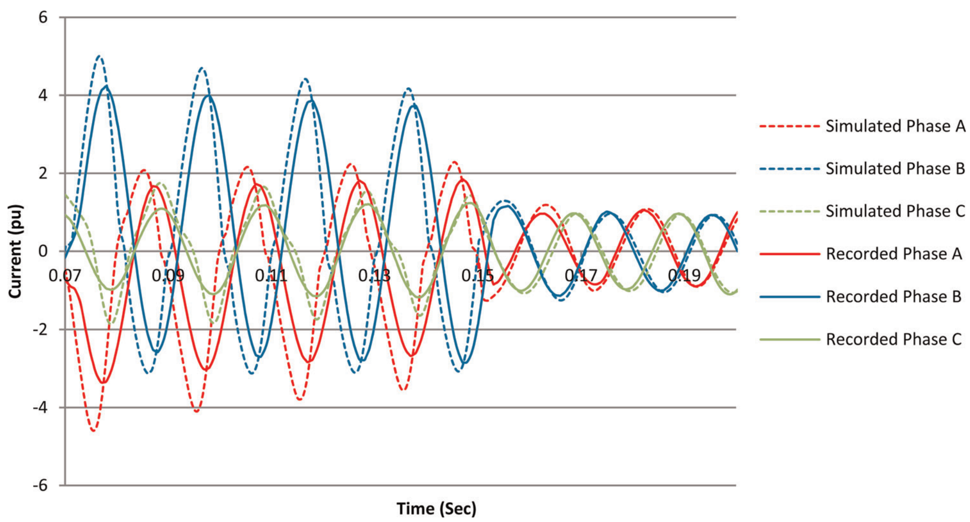

Fig. 9 *Stator currents calculated with final identified parameter values compared with the recorded transient*

IET Gener. Transm. Distrib., pp. 1–8

itself (stage 1), the parameter identification process is more difficult because of the nature of the event itself (a remote line-to-line fault and not a three-phase balanced fault or even a line-to-line fault at the generator terminals) giving network and multi-machine interactions whose effects cannot be accurately modelled. On the other hand, conditions during the fault clearance stage are more precise and consistent. The clearance of the fault limits the influence of the external network and allows the model (and hence the identified parameters) to reflect the real situation more accurately. Calculated over the entire period of the recorded transient, an integral current error value of 0.007 pu was obtained with the final identified parameters (Fig. 9) compared with 0.021 pu for the manufacturer's values set (Fig. 7), giving confidence in the accuracy of the PSO identified parameter values.

7 Conclusion

A non-invasive turbo-generator parameter identification method based on particle swarm optimisation that is capable of identifying generator, exciter and turbine parameters using recorded network transient data from a 178 MVA 2-pole, 18 kV steam turbine generator is presented in this paper. The multistage process allows for the identification of a large number of parameters in a format that is computationally efficient. Using industry standard models for the generator, turbine and excitations system, the PSO identified parameters produce a calculated response of the synchronous generator that gives a good overall match with the recorded network data, giving confidence in the accuracy of the proposed parameter identified process.

8 References

1 Say, M.G.: 'Alternating current machines' (John Wiley & Sons, 1984)
2 Arjona, M.A., Cisneros-González, M., Hernandez, C.: 'Parameter estimation of a synchronous generator using a sine cardinal perturbation and mixed stochastic–deterministic algorithms', *IEEE Trans. Ind. Electron.*, 2011, **58**, (2), pp. 486–493
3 Vandoorn, T.L., de Belie, F.M., Vyncke, T.J., Melkebeek, J.A., Lataire, P.: 'Generation of multisinusoidal test signals for the identification of synchronous machine parameters by using a voltage-source inverter', *IEEE Trans. Ind. Electron.*, 2010, **57**, (1), pp. 430–439
4 Wamkeue, R., Baetscher, F., Kamwa, I.: 'Hybrid-state-model time-domain identification of synchronous machine parameters from saturated load rejection test records', *IEEE Trans. Energy Convers*, 2008, **23**, (1), pp. 68–77
5 Wamkeue, R., Kamwa, I., Dai-Do, X.: 'Short-circuit test based maximum likelihood estimation of stability model of large generators', *IEEE Trans. Energy Convers*, 1999, **14**, (2), pp. 167–174
6 IEEE Std 421.5–2006: 'IEEE Recommended Practice for Excitation System Models for Power System Stability Studies', IEEE, 2006
7 Underwood, S.J., Husain, I.: 'Online parameter estimation and adaptive control of permanent-magnet synchronous machines', *IEEE Trans. Ind. Electron.*, 2010, **57**, (7), pp. 2435–2443
8 Vermeulen, H.J., Strauss, J.M., Shikoana, V.: 'Online estimation of synchronous generator parameters using PRBS perturbations', *IEEE Trans. Power Syst.*, 2002, **17**, (3), pp. 694–700
9 Huang, J., Corzine, K.A., Belkhayat, M.: 'Online synchronous machine parameter extraction from small-signal injection techniques', *IEEE Trans. Energy Convers*, 2009, **24**, (1), pp. 43–51
10 Zhoa, Z., Zheng, F., Gao, J., Xu, L.: 'A dynamic on-line parameter identification and full-scale system experimental verification for large synchronous machines', *IEEE Trans. Energy Convers*, 1995, **10**, (3), pp. 392–398
11 Karayaka, H.B., Keyhani, A., Heydt, G.T., Agrawal, B.L., Selin, D.A.: 'Synchronous generator model identification and parameter estimation from operating data', *IEEE Trans. Energy Convers*, 2003, **18**, (1), pp. 121–126
12 Nagpal, M., Moshref, A., Morison, G.K., Kundur, P.: 'Experience with testing and modelling of gas turbines'. IEEE Power Engineering Society Winter Meeting, 2001, vol. 2, pp. 652–656
13 Dandeno, P.L., Kundur, P., Poray, A.T., Coultes, M.E.: 'Validation of turbo generator stability models by comparisons with power system tests', *IEEE Trans. Power Appar. Syst.*, 1981, **100**, pp. 1637–1645
14 Ong, C.: 'Dynamic simulation of electric machinery using Matlab/Simulink' (Prentice Hall, 1997)
15 IEEE Committee Report: 'Dynamic models for steam and hydro turbines in power system studies', *IEEE Trans. Power Appar. Syst.*, 1973, **92**, pp. 1904–1915
16 IEEE Std 1110–2002: 'IEEE Guide For Synchronous Generator Modeling Practices and Applications in Power System Stability Analyses', IEEE, 2002
17 Working group on Prime Mover and Energy Supply Models for System Dynamic Performance Studies: 'dynamic models for fossil fueled steam turbine units in power system studies', *IEEE Trans. Power Syst.*, 1991, **6**, (2), pp. 753–761
18 Del Valle, Y., Venayagamoorthy, G.K., Mohagheghi, S., Hernandez, J.C., Harley, R.G.: 'Particle swarm optimization: basic concepts, variants and applications in power systems', *IEEE Trans. Evol. Comput.*, 2008, **12**, pp. 171–195
19 Saxena, D., Bhaumik, S., Singh, S.N.: 'Identification of multiple harmonic sources in power system using optimally placed voltage measurement devices', *IEEE Trans. Ind. Electron.*, 2014, **61**, (5), pp. 2483–2492
20 Jain, N., Singh, S.N., Srivastava, S.C.: 'A generalized approach for DG planning and viability analysis under market scenario', *IEEE Trans. Ind. Electron.*, 2013, **60**, (11), pp. 5075–5085
21 Ishaque, K., Salam, Z.: 'A deterministic particle swarm optimization maximum power point tracker for photovoltaic system under partial shading condition', *IEEE Trans. Ind. Electron.*, 2013, **60**, (8), pp. 3195–3206
22 Shen, K., Zhao, D., Mei, J., *et al.*: 'Elimination of harmonics in a modular multilevel converter using particle swarm optimization based staircase modulation strategy', *IEEE Trans. Ind. Electron.*, 2014, **61**, (10), pp. 5311–5322
23 Hasanien, H.M.: 'Particle swarm design optimization of transverse flux linear motor for weight reduction and improvement of thrust force', *IEEE Trans. Ind. Electron.*, 2011, **58**, (9), pp. 4048–4056
24 Bracikowski, N., Hecquet, M., Brochet, P., Shirinskii, S.V.: 'Multiphysics modeling of a permanent magnet synchronous machine by using lumped models', *IEEE Trans. Ind. Electron.*, 2012, **59**, (6), pp. 2426–2437
25 El-Naggar, K.M., Al-Othman, A.K., Al-Sumait, J.S.: 'A particle swarm digital identification of synchronous machine parameters from short circuit tests'. IASTED Int. Conf. on artificial intelligence and soft computing, August 2006
26 Li, Q., Chen, W., Wang, Y., Liu, S., Jia, J.: 'Parameter identification for PEM fuel-cell mechanism model based on effective informed adaptive particle swarm optimization', *IEEE Trans. Ind. Electron.*, 2011, **58**, (6), pp. 2410–2419
27 Lin, W., Su, T., Wu, R.: 'Parameter identification of induction machine with a starting no-load low-voltage test', *IEEE Trans. Ind. Electron.*, 2012, **59**, (1), pp. 352–360
28 Yin, P., Wang, J.: 'A particle swarm optimization approach to nonlinear resource allocation problem', *Appl. Math. Comput.*, 2006, **183**, pp. 232–242
29 Clerc, M.: 'Particle swarm optimisation' (ISTE Ltd, London, 2006)

9 Appendix

As stated above, the parameters of the machine model used in the analysis (i.e. R_{kq}, X_{lkq}, R_{kd}, X_{lkd}, R_f, X_{md} and X_{lf} in (1)–(8)) are not in a form which relates directly to the parameters normally available from generator manufacturers (i.e. machine armature resistance, direct and quadrature axes reactances, transient and sub-transient reactances and time constants etc.) that are the subject of the parameter identification process. However, the two sets of parameters are related by the following set of equations, as detailed in [14].

The field leakage reactance X_{lf} is given by

$$X_{lf} = \frac{X_{md}(X_d - X_{ls})}{X_{md} - (X_d - X_{ls})}$$

where X_{ls} is the armature leakage reactance normally given by manufacturers and X_{md} is the direct axis magnetising reactance obtained by subtracting the leakage reactance from the direct axis reactance X_d

$$X_{md} = X_d - X_{ls}$$

The leakage reactance of the d-axis damper winding X_{lkd} is given by

$$X_{lkd} = \frac{(X''_d - X_{ls})X_{md}X_{lf}}{X_{lf}X_{md} - (X''_d - X_{ls})(X_{md} + X_{lf})}$$

where X''_d is the direct axis sub-transient reactance.

And the leakage reactance of the q-axis damper winding X_{lkq} is given by

$$X_{lkq} = \frac{X_{mq}(X''_q - X_{ls})}{X_{mq} - (X''_q - X_{ls})}$$

where X''_q is the quadrature axis sub-transient reactance and X_{mq} is the is the quadrature axis magnetising reactance obtained by subtracting the leakage reactance from the q-axis reactance X_q

$$X_{mq} = X_q - X_{ls}$$

The field resistance R_f and the rotor winding resistances R_{kd}, R_{kq} can be calculated from the machine time constants, as follows

$$R_f = \frac{1}{\omega_b T'_d}(X_{lf} + X_{md})$$

$$R_{kd} = \frac{1}{\omega_b T''_d}(X_{lkd} + X_d + X_{ls})$$

$$R_{kq} = \frac{1}{\omega_b T''_q}(X_{lkq} + X_{mq})$$

where T'_d is the d-axis transient time constant and T''_d, T''_q are the d-axis and q-axis sub-transient time constants, respectively.